JPn Neuroscience
The Journal of Physiology



# Residues in the pore region of *Drosophila* transient receptor potential A1 dictate sensitivity to thermal stimuli

Hong Wang, Melanie Schupp, Sandra Zurborg and Paul A. Heppenstall

*Mouse Biology Unit, European Molecular Biology Laboratory (EMBL), Via Ramarini 32, 00015 Monterotondo, Italy*

**Key points**

- Transient receptor potential (TRP) A ion channels are evolutionarily conserved and play a fundamental role in thermal, chemical and mechanical transduction.
- In this study, we characterized *Drosophila* TRPA1 as a non-selective cation channel that can be activated by heat, voltage and chemicals.
- By constructing the chimeric channel between *Drosophila* TRPA1 and its cold-sensitive human orthologue, we identified key residues in the transmembrane domain that confer heat sensitivity.
- Perturbation of the putative voltage-sensing module increased the threshold for heat activation.
- Single channel recordings revealed the reaction schemes of wild-type and mutant channels.

**Abstract** The capacity to sense temperature is essential for the survival of all animals. At the molecular level, ion channels belonging to the transient receptor potential (TRP) family of channels function as temperature sensors in animals across several phyla. TRP channels are opened directly by changes in temperature and show pronounced sensitivity at their activation range. To determine how temperature activates these channels, we analysed channels belonging to the TRPA family, which detect heat in insects and cold in mammals. By constructing chimeric proteins consisting of human and *Drosophila* TRPA1 channels, we mapped regions that regulate thermal activation and identified residues in the pore helix that invert temperature sensitivity of TRPA1. From analysis of individual channels we defined the gating reaction of *Drosophila* TRPA1 and determined how mutagenesis alters the energy landscape for channel opening. Our results reveal specific molecular requirements for thermal activation of TRPA1 and provide mechanistic insight into this process.

(Resubmitted 10 August 2012; accepted 25 September 2012; first published online 1 October 2012)
**Corresponding author** P. A. Heppenstall: Mouse Biology Unit, European Molecular Biology Laboratory (EMBL), Via Ramarini 32, 00015 Monterotondo, Italy. Email: paul.heppenstall@embl.it

**Abbreviations** TRP, transient receptor potential; $Z_{app}$, apparent gating charge.


DOI: 10.1113/jphysiol.2012.242842

## Introduction

Temperature detection is dependent upon specialized sensory neurons that detect small changes in environmental temperature and signal to neuronal circuits to elicit an appropriate response (McKemy, 2007). Several transient receptor potential (TRP) channels have emerged as candidate receptor molecules for temperature based upon their expression by sensory neurons and robust activation by temperature (Patapoutian *et al.* 2003). Different subtypes of TRP channels are activated at distinct temperatures allowing for the detection of small changes in environmental temperature over a broad physiological range. In mammals, channels belonging to the TRPV family detect warmth, TRPM8 is the principal cool sensor, and the sole mammalian member of the TRPA family, TRPA1, is activated by prolonged cold exposure (Patapoutian *et al.* 2003).

TRPA channels represent an intriguing example of the functional diversity of TRP channels. In addition to their function as temperature detectors, these channels have a highly conserved role in chemical nociception owing to their activation by reactive electrophiles (Bautista *et al.* 2006; Kang *et al.* 2010). Remarkably, TRPA channels have also evolved distinct temperature sensitivity in several animal species. In mammals, they act as cold sensors, whereas in flies and some species of snake, they function as heat sensors. Thus in *Drosophila*, the TRPA subfamily includes three heat-sensitive channels: Painless (Tracey *et al.* 2003), Pyrexia (Lee *et al.* 2005) and *Drosophila* TRPA1 (dTRPA1) (Viswanath *et al.* 2003; Hamada *et al.* 2008), which are opened at temperatures between 25°C and 45°C. Similarly, in snakes, TRPA1 responds to temperatures of about 27°C and has been implicated in the detection of infrared radiation (Gracheva *et al.* 2010). These findings indicate that mammals, snakes and flies have independently adapted TRPA channels to detect discrete temperatures and that potentially, common mechanisms could underlie their thermal sensitivity. Given the significant sequence similarity between human and dTRPA1, we reasoned that TRPA channels could serve as a model system for defining the structures required for activation of ion channels by temperature.

Here we utilized an approach based upon the generation and evaluation of chimeric *Drosophila*/human TRPA1 channels to map thermo-responsive regions. We identified single amino acids in the transmembrane region of dTRPA1 that dictate the temperature sensitivity of the channel, and from analysis of individual channels we determined how mutagenesis modifies the gating reaction of the channel and disrupts thermal activation.

## Methods

### Molecular biology and cell culture

Reliable expression of *Drosophila* ion channels is notoriously difficult to achieve in commonly used mammalian cell expression systems. We found that *Drosophila* S2 cells permit robust expression of dTRPA1, allowing culture below activation temperatures of dTRPA1 and promoting functional expression as confirmed by high sensitivity of channels to heat and chemical activators (Supplementary Fig. S1*A*–*C*).

All *Drosophila*-based channels and chimeras were based upon the highly temperature-dependent canonical TRPA1 isoform (Viswanath *et al.* 2003). Constructs were cloned into the *Drosophila* expression vector, pMT/V5-His, containing the inducible metallothionein gene promoter (Invitrogen, Darmstadt, Germany). *Drosophila* S2 cells were acquired from Invitrogen and maintained according to the manufacturer's protocol at 25°C. Cells were transiently transfected with channel and a yellow fluorescent protein reporter plasmid using FugeneHD (Roche, Mannheim, Germany) at a ratio of 3:1. Twenty-four hours later, expression was initiated using 500 $\mu$M $CuSO_4$ and cells were used for experiments after a further 16–24 h of incubation. All experiments were repeated with at least three different transfections. For control cells, yellow fluorescent protein was transfected with empty vector.

Chimeric channels were constructed using the In-Fusion-based PCR cloning system (Clontech, Mountain View, CA, USA). PCR fragments of channel with vector backbone and chimeric insert were generated with 15 bp regions of homology at the 3′ and 5′ ends. Vector and insert were combined following the manufacturer's protocol (Clontech). Point mutagenesis was performed using the QuikChange II XL kit according to the manufacturer's protocol (Agilent, Santa Clara, USA). All mutations were verified by sequencing.

For V5 epitope staining, cells were fixed with paraformaldehyde, permeabilized with triton and sequentially incubated with mouse monoclonal anti-V5 antibody (Sigma, Hamburg, Germany) and Alexa Fluor 555 goat anti-mouse IgG (Invitrogen). Cells were mounted on glass slides and imaged with a fluorescent microscope (Leica, Wetzlar, Germany).

### Calcium imaging

Ratiometric calcium imaging was performed using FURA-2 AM dye (Invitrogen) and analysed using Tillvision software (Till Photonics, Munich, Germany). Transfected cells were plated on glass coverslips, loaded with 3 $\mu$M Fura-2 AM in calcium imaging buffer (120 mM NaCl, 5 mM KCl, 2 mM $CaCl_2$, 4 mM $MgCl_2$, 10 mM Tes,

40 mM sucrose, 2.5 mM probenecid, pH 7.2 adjusted with NaOH) and placed in a recording chamber that allowed direct application of buffer at controlled temperature (ESF Electronic, Goettingen, Germany). Fluorescence was measured at excitation wavelengths alternating between 340 nm and 380 nm. Following subtraction of background fluorescence, the ratio of fluorescence at 340 nm and 380 nm was calculated. All graphs are averaged ratios of 50–200 individual cells.

## Electrophysiology

Gigaseals were formed with pipettes that had a resistance between 4 and 6 MΩ in standard pipette solution. For whole cell recordings, bath solution contained 135 mM NaCl, 5.4 mM CsCl, 1.8 mM $CaCl_2$, 1 mM $MgCl_2$, 10 mM glucose and 5 mM Hepes, pH 7.2. Pipette solution contained 20 mM CsCl, 120 mM caesium aspartate, 0.01 mM $CaCl_2$, 2 mM $MgCl_2$, 1 mM EGTA, 1 mM $Na_2ATP$ and 5 mM HEPES, pH 7.2. The calculated free $Ca^{2+}$ concentration was 100 nM.

Whole cell membrane currents were monitored using an EPC-10 patch-clamp amplifier and Patchmaster software (HEKA Elektronic, Lambrecht, Germany). All voltages were corrected for a liquid junction potential of 15 mV (S2 cells) using the Henderson equation (Barry & Diamond, 1970). Capacitance and access resistance were continuously monitored and between 10 and 50% of the series resistance was compensated. Data were sampled at 10–20 kHz and filtered at 2–5 kHz.

Slow temperature ramps were applied using a Peltier device (ESF Electronic, Germany) that changed the temperature of the superfusing buffer at $1^{\circ}C\,s^{-1}$. The temperature was monitored with a thermocouple placed within the flow of buffer and close to the cells. To measure heat activation of channels, cells were held at −30 mV for 20 ms, stepped to −100 mV for 10 ms and ramped to +100 mV ($0.5\,mV\,ms^{-1}$) every 5 s for 400 s during which time the temperature was raised and then cooled back to baseline. Current amplitude was extracted at −100 mV and +100 mV for each ramp over the temperature range. We observed that repeated heating in the presence of $Ca^{2+}$ led to desensitization. We therefore selected cells for analysis based upon the following rules. First, only cells that recovered fully to baseline after heating and cooling were chosen. Secondly, to avoid the effect of desensitization, we analysed only the response to the first heat stimulus and recorded no more than three cells per plate. Thirdly, channels were judged to be functionally expressed based upon their response to voltage with a threshold of 100 pA at 100 mV and the presence of a clearly outwardly rectifying current.

Relative permeability ratios were determined by replacing $Na^+$ with test ions in the bath solution while applying voltage ramps at 32°C. For monovalent cations, bath solution contained 140 mM NaCl or 140 mM KCl or 140 mM CsCl, with 10 mM glucose and 10 mM HEPES. pH was adjusted to 7.2 with NaOH, KOH or CsOH, respectively, and junction potentials were compensated as follows: 16 mV for $Na^+$, 10 mV for $K^+$, 10 mV for $Cs^+$. For divalent cations, bath solutions consisted of 90 mM NaCl, 10 mM glucose, 10 mM HEPES, 30 mM $CaCl_2$ (or $MgCl_2$) and pH was adjusted to 7.2 with NaOH. Junction potentials were compensated at 18 mV. Voltage ramps from −100 mV to 80 mV were applied for 2 s to measure the reversal potential. For monovalent ions, permeability ratios to sodium ion: $Na^+$ ($P_X/P_{Na}$) were calculated according to

$$\frac{P_X}{P_{Na}} = e^{(V_X - V_{Na})\frac{F}{RT}}$$

where $V_X$–$V_{Na}$ is the reversal potential change, $F$ the Faraday constant, $R$ the universal gas constant and $T$ the absolute temperature. For divalent cations, ratios were calculated according to

$$\frac{P_X}{P_{Na}} = \frac{1 + e^{\beta_x}}{4[X]_o}\{[Na]_{o1}e^{\beta_x - \beta_{Na}} - [Na]_o\},$$

where $\beta_x = \frac{V_x F}{RT}$).

To measure whole cell voltage-dependent activation of channels, families of voltage-activated currents were acquired at defined temperatures. These consisted of 200 ms voltage steps from −120 mV to 200 mV in 20 mV increments followed by a 50 ms step at −120 mV. Data were extracted only from cells that underwent testing across the full temperature range. Conductance was calculated from the steady-state current and plotted against voltage. Data were fitted with single Boltzmann functions

$$\left(P_{open} = \frac{1}{1 + \exp(-\frac{zF(V - V_{1/2})}{RT})}\right).$$

Single channel recordings were made in the inside-out or cell-attached configuration using gigaseals larger than 10 GΩ and were acquired with an EPC-10 patch-clamp amplifier and Patchmaster software (HEKA Elektronic, Germany). Inside-out recordings were used to measure unitary conductance and plot single channel $I$–$V$ curves. Bath solution contained 140 mM caesium aspartate, 10 mM EGTA, 10 mM HEPES and 0.4 mM $CaCl_2$, (pH 7.2). Pipette solution contained 140 mM caesium aspartate, 10 mM EGTA, 1 mM $MgCl_2$ and 5 mM HEPES, (pH 7.2). Cell-attached configuration was used to record extended traces for kinetic analysis. The bath solution contained 120 mM KCl, 5 mM HEPES, 1 mM $MgCl_2$ and 2 mM $CaCl_2$ (pH 7.2) and the pipette solution contained 100 mM KCl, 10 mM HEPES, 1 mM $MgCl_2$ and 10 mM EGTA (pH 7.2).

Single channel data were sampled at 20 kHz and filtered at 3 kHz.

Only long recordings showing activity of single channels were selected for kinetic analysis. Traces were visually inspected to exclude those with low signal-to-noise, artifacts and run-down or desensitization of currents. Baseline drift was corrected manually. Data were analysed using the QuB software package (www.qub.buffalo.edu) and idealized with the segmental k-means algorithm (Qin, 2004). Following manual inspection of idealization, dwell-time histograms were constructed and fitted with sums of exponentials using a maximum likelihood routine. A dead time of 100 $\mu$s corresponding to the 10–90% rise time of the filtered record was imposed upon each trace.

To evaluate kinetic models for each channel we used the maximum interval likelihood (MIL) method (Qin *et al.* 1997) to fit different kinetic schemes of increasing complexity. Both the model search function of QuB and manual generation of models were employed to ensure that we tested all possible non-cyclic arrangements that corresponded to the number of exponentials calculated from dwell-time histograms. In total this amounted to several hundred schemes for each channel, which were ranked according to their log likelihoods and by visual inspection of fitted data. Additionally, for the H990A-R1004N mutant channel, data were idealized using both an open-subconductance-closed model and an open-closed model (where the subconductance state was combined with the open state). Kinetic schemes were evaluated for each idealization, and in all cases, the open-subconductance-closed model fitted the data more adequately. For each channel, the five highest ranking models with their rates are displayed in Supplementary Table S1.

To simulate temperature dependent single channel responses for dTRPA1 and H990A-R1004N we first generated global models for each channel. Data obtained at 24°C and 32°C for dTRPA1 or 34°C and 40°C for H990A-R1004N were simultaneously fitted with Scheme 1 for each channel using the MIL method. All rate constants were allowed to vary and temperature dependence was calculated using the equation

$$K(T) = k_0 \cdot T \cdot \exp(k_1/T)$$

where $K(T)$ is the rate constant at temperature $T$, $k_0$ is the pre-exponential rate constant, $T$ is the absolute temperature, and $k_1$ is the exponential rate constant. Single channel currents were simulated by applying these parameters to the simulator function of QuB software at a sampling rate of 20 kHz filtered at 3 kHz. Temperature ramps (and $1/T$ ramps) were generated from 15°C to 45°C at 0.2°C s$^{-1}$.

## Results

### Characterization of heterologously expressed *Drosophila* transient receptor potential A1

Reliable expression of *Drosophila* ion channels is notoriously difficult to achieve in commonly used mammalian cell expression systems and has prevented analysis of many of these channels at the cellular level. We found that *Drosophila* S2 cells permit robust expression of dTRPA1 and serve as an excellent system for biophysical characterization of *Drosophila* channels. Using this system, we were able to culture cells at room temperature and achieve high levels of membrane expression (Supplementary Fig. S1*A*). Furthermore, dTRPA1 was strongly activated by the electrophilic compounds formalin and allylisothiocyanate (Supplementary Figs. S1*B* and *C*) at concentrations similar to those that activate mammalian channels (Bandell *et al.* 2004; Jordt *et al.* 2004), demonstrating robust functional expression of the channel.

We characterized the biophysical properties of dTRPA1 activation using whole cell patch clamping. Heating of dTRPA1 transfected cells from room temperature to 35°C evoked a large outwardly rectifying current (Fig. 1*A* and *B*) with a temperature coefficient ($Q_{10}$) of 8.5 at −100 mV and 3.7 at +100 mV. The values are lower than those reported for other heat-responsive TRP channels (Jordt *et al.* 2003) and may reflect channel desensitization during slow temperature ramps. dTRPA1 current reversed at close to 0 mV and ion substitution experiments revealed that dTRPA1, like its human counterpart, is a non-selective cation: channel with little discrimination among monovalent or divalent ions (Story *et al.* 2003) (Supplementary Fig. S1*D*, relative permeabilities: $P_K/P_{Na} = 1.1$, $P_{Cs}/P_{Na} = 1.1$, $P_{Mg}/P_{Na} = 1.1$, $P_{Ca}/P_{Na} = 1.7$).

The pronounced outward rectification of dTRPA1 is reminiscent of activation of mammalian thermally gated TRP channels and indicated a voltage dependence of the channel (Nilius *et al.* 2005). Indeed, plotting current against temperature shows that dTRPA1 has a steep temperature dependence that shifts at positive voltage to allow the channel to be activated at lower temperatures (Fig. 1*B*). We examined voltage dependence of dTRPA1 by applying a voltage step protocol ranging from −120 mV to 200 mV at different temperatures (Fig. 1*C*). Similarly to human TRPA1 (hTRPA1) (Zurborg *et al.* 2007), the *Drosophila* channel was readily activated by voltage but with significantly faster kinetics than the human orthologue (time constant of activation for dTRPA at 60 mV and 28°C, 5.9 ± 1.4 ms, for hTRPA1, 18.4 ± 4 ms) and negligible tail currents (Fig. 1*C*).

Voltage-dependent regulation of TRP channels has been explored extensively for mammalian thermally gated channels and revealed that in addition to a

role for voltage in modulating temperature thresholds, temperature induces a leftward shift in voltage activation towards physiologically relevant potentials (Brauchi *et al.* 2004; Voets *et al.* 2004, 2007; Nilius *et al.* 2005; Talavera *et al.* 2005; Karashima *et al.* 2009). We analysed dTRPA1 and found that increasing temperature induced a shift in the voltage activation curve (half-maximal activation ($V_{1/2}$) at 24°C: 146.4 ± 5.1 mV, and at 32°C: 63.5 ± 3.4 mV) and increased the maximal conductance of the channel (Fig. 1*D*), implying that voltage and temperature may share common mechanisms in channel gating. We reasoned that by identifying and altering the structures in dTRPA1 that govern thermosensitivity, we would be able to test this assumption and uncover mechanisms that lead to channel activation.

## Mapping the heat sensor in *Drosophila* transient receptor potential A1

To identify the heat sensor in dTRPA1, we initially sought to screen the full length of the channel by generating chimeras of human and dTRPA1. As a first step in this process, we re-examined the temperature sensitivity of hTRPA1. hTRPA1 was not activated by heating (Supplementary Fig. S2*A*); however, cooling to 13°C induced a leftward shift of the voltage activation curve (Supplementary Fig. S2*B*) as reported previously (Karashima *et al.* 2009). This indicates that hTRPA1 can be weakly activated by cold and analysis of its voltage dependence is a sensitive method to detect this modulation. On the basis of structural

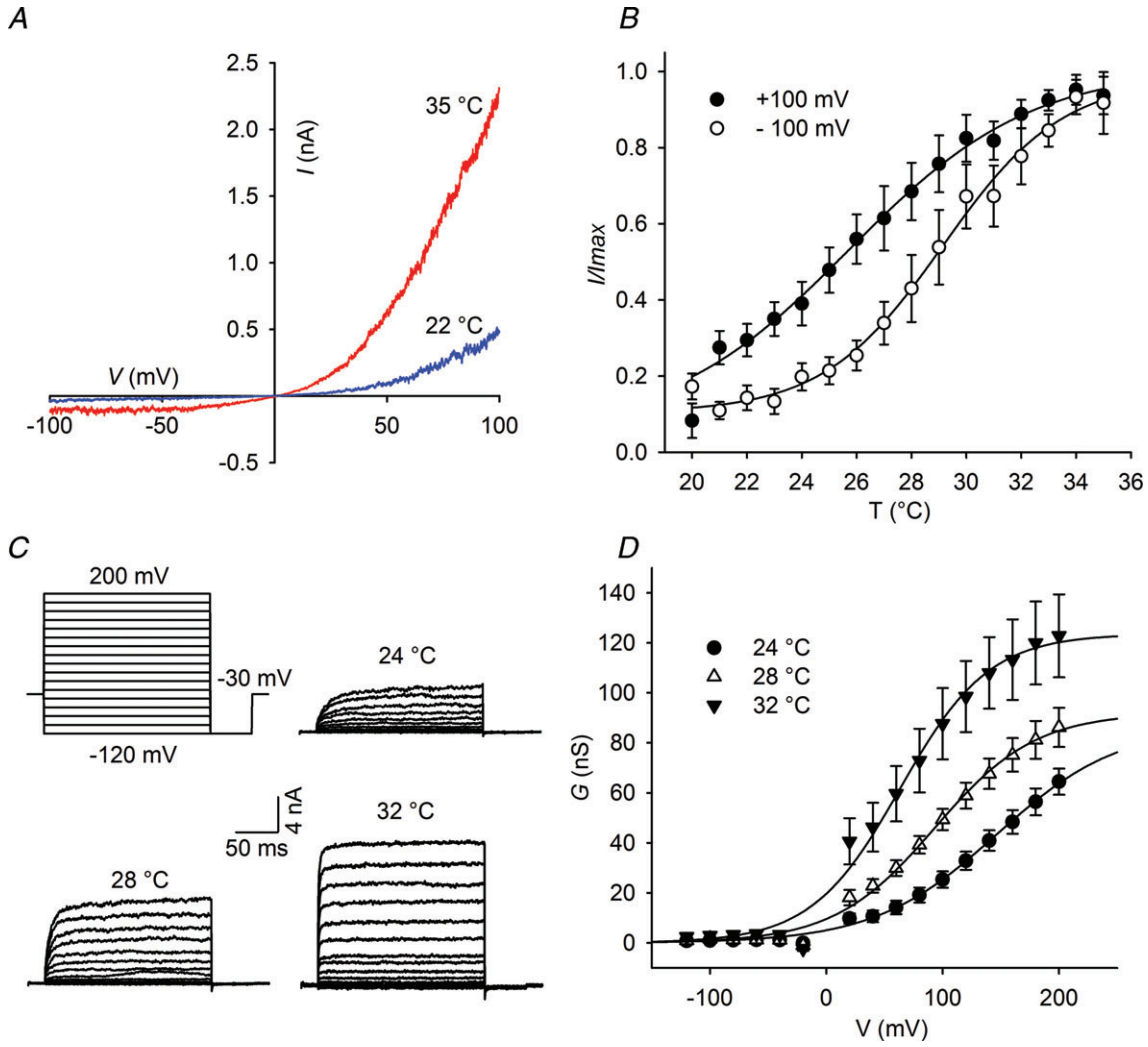


**Figure 1. Activation of *Drosophila* transient receptor potential A1 (dTRPA1) by heat and voltage**
*A*, voltage ramps from −100 mV to +100 mV evoke an outward rectifying current in dTRPA1 that is potentiated at warm temperatures. *B*, dTRPA1 is activated by temperature in the range 20–35°C. Positive voltage shifts the temperature activation curve to the left ($n = 11$). *C*, current traces of dTRPA1 at indicated temperatures in response to the voltage protocol at the upper left. *D*, voltage-dependent activation of dTRPA1 at 24°C ($n = 14$), 28°C ($n = 13$) and 32°C ($n = 8$). Continuous lines are best fits to Boltzmann functions. Data are expressed as means ± SEM.

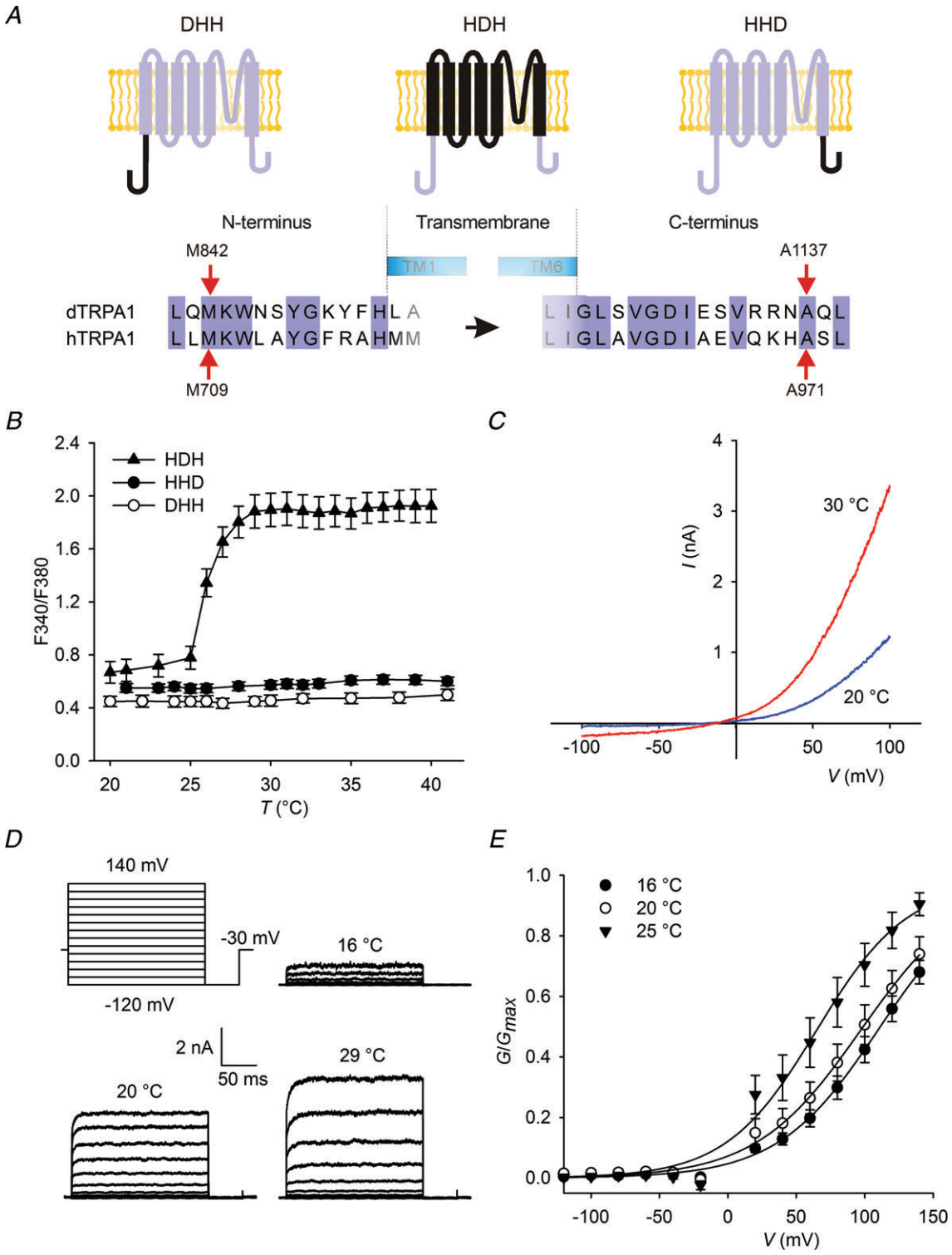


**Figure 2. Activation of HDH chimeric channels by heat and voltage**
*A*, schematic diagram of chimera construction. *B*, increasing temperature raises intracellular calcium concentration in HDH expressing cells. *C*, *I–V* curves of HDH channels. *D*, current traces of HDH chimeras at different temperatures in response to the voltage protocol indicated at the upper left. *E*, voltage-dependent activation of HDH at 16°C ($n = 8$), 20°C ($n = 6$) and 25°C ($n = 7$). dTRPA1, *Drosophila* transient receptor potential A1; hTRPA1, human TRPA1.

predictions, we next arbitrarily divided the channel into N-terminal, transmembrane and C-terminal domains and constructed chimeric TRPA channels consisting of all possible combinations of these regions (termed DHH, HDH, HHD, etc, Fig. 2*A*). As illustrated in Supplementary Fig. S3, chimeras were correctly trafficked and inserted into the plasma membrane of S2 cells. We then used calcium imaging to assay heat-induced increases in calcium influx in these cells. Strikingly, we observed that inclusion of only the transmembrane region of dTRPA1 (HDH) was sufficient to induce heat activation of the human channel and thus reverse thermal sensitivity (Fig. 2*B*). We analysed the HDH chimeric channel further using whole cell patch clamping. HDH displayed a prominent outward rectifying current that was comparable to dTRPA1 (Fig. 2*C*). Voltage-dependent currents were also evident and raising temperature shifted the activation curve to the left (Fig. 2*D* and *E*).

We assumed that one or more structures must be present within the transmembrane region, which account for heat sensitivity of dTRPA1. To locate potential structures we aligned amino acid sequences covering this region from several *Drosophila* and mammalian species (Supplementary Fig. S4). Two areas were clearly distinct in dTRPA1; a stretch of additional residues between transmembrane region 1 (S1) and S2, and a smaller insertion following S5. We first examined the region between S1 and S2. It is predicted to extend extracellularly and contains two well-conserved cysteine residues in dTRPA1 that we reasoned might form a disulphide bond (Fig. 3*A*, C891 and C917). We treated HDH channels with reducing agent *tris*(2-carboxyethyl) phosphine (data

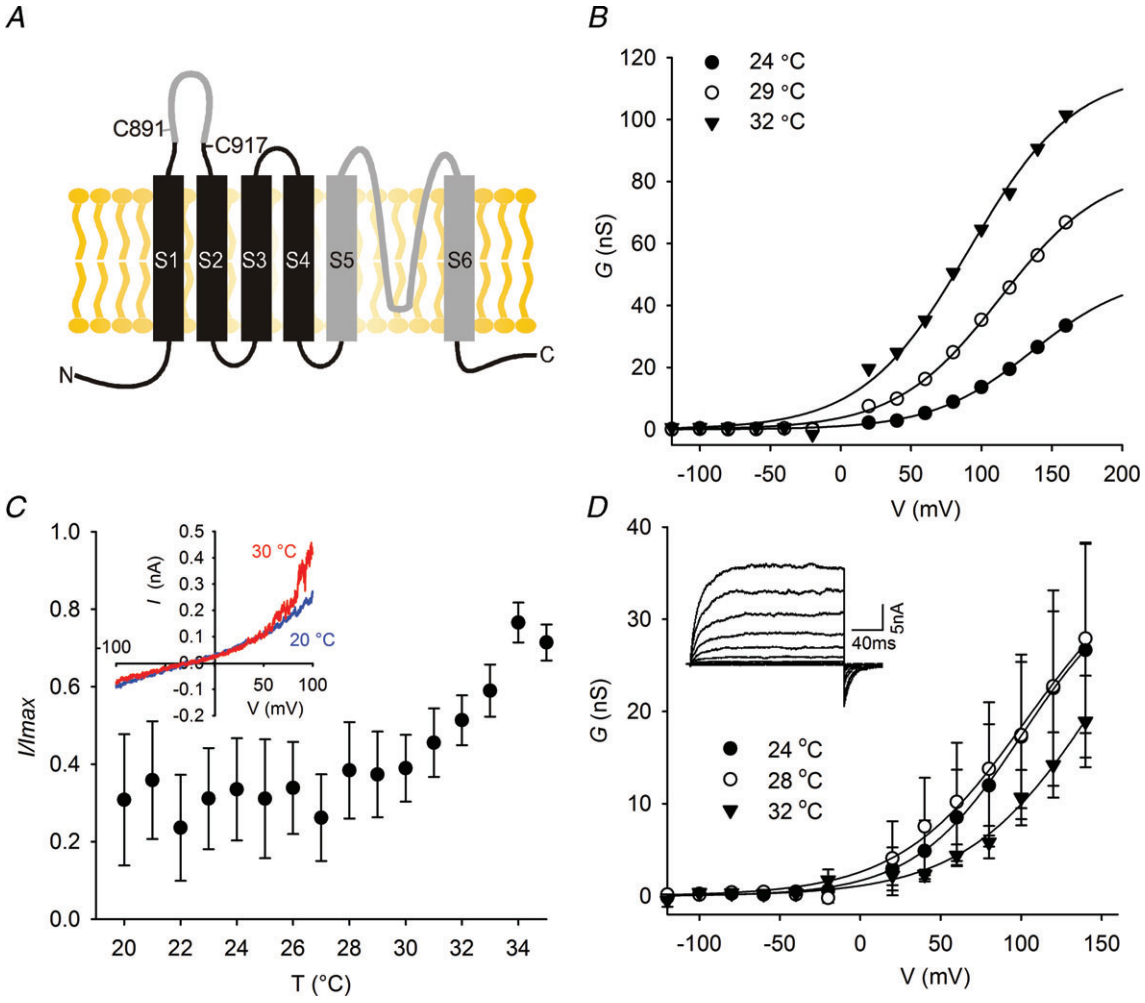


**Figure 3. A thermoregulatory module of *Drosophila* transient receptor potential A1 (dTRPA1) locates to the pore region**
*A*, schematic diagram of dTRPA1 showing regions exchanged with human sequence in grey. *B*, deletion of the insertion between S1 and S2 in dTRPA1 does not alter temperature or voltage sensitivity. *C*, replacing S5–S6 in dTRPA1 with human counterpart abolishes heat activation (inset shows *I–V* curve). *D*, voltage-dependent activation of HDH-H56 is not altered by increasing temperatures (inset shows representative whole cell current traces at 24°C) (24°C, $n = 7$; 28°C, $n = 8$; 32°C, $n = 7$).

not shown), mutated both cysteine residues to serines (Supplementary Fig. S5*A*), and deleted the whole of this region in HDH so that it resembled hTRPA1 (Fig. 3*B*, ΔG882–S916). Surprisingly, none of these perturbations had any effect on heat or voltage sensitivity of the channel, suggesting that this insert is a result of speciation in *Drosophila* but has little functional importance for channel gating.

We next analysed the region following S5 in HDH and dTRPA1 by exchanging all *Drosophila* sequence from the beginning of S5 to the end of S6 with human sequence (Supplementary Fig. S4, from L1026 to A1137, termed dTRPA1-H56 and HDH-H56). Heat sensitivity was strongly reduced in dTRPA1-H56 and HDH-H56 (Fig. 3*C* and *D*) and thermal activation was significantly lower than for dTRPA1 and HDH. Mutant channels displayed voltage dependence and strikingly, prominent tail currents were evident, reminiscent of those observed in hTRPA1 (Zurborg *et al.* 2007) (Fig. 3*D* inset). Raising temperature did not induce a shift in the voltage activation curve as observed with dTRPA1 and HDH (Fig. 3*D*).

## Mutations in the *Drosophila* transient receptor potential A1 pore influence temperature sensitivity

The TRP channel pore is predicted to lie between S5 and S6 and we reasoned that by substituting apparent structural units here in dTRPA1 with corresponding sequences from hTRPA1, we would achieve broader sequence coverage than from single point mutagenesis. We therefore divided the pore into turret, helix, post-filter and S6 regions (Fig. 4*A*) and used patch clamping to determine changes in heat activation. Replacement of the pore turret and post-filter had no effect on thermal sensitivity (Fig. 4*B* and *C*); however, exchange of S6 (Fig. 4*D*) and the pore helix (Fig. 4*E*) strongly reduced temperature sensitivity.

We next mutated residues in S6 and the helix of HDH to their equivalents in hTRPA1. We assumed that some of the differences between human and *Drosophila* channels might reflect changes in the position of structurally important residues such as the hydrophobic VS to SV in S6 and the helix-breaking proline at position 1068 in the pore helix. In designing mutations, we therefore attempted to transfer these orientations, often using double rather than single mutations (Fig. 5*A* and *B*). In agreement with our data from chimeric channels, point mutations in S6 reduced heat sensitivity (Fig. 5*C*, Supplementary Fig. 5*B*, and data not shown), while in the pore helix we observed dramatic effects on temperature activation; R1073Q and N1066+I1067 to S (Fig. 5*D*, Supplementary Fig. S5*C*) mutants displayed a small increase in activity at colder temperatures and positive potentials. Similarly, the charge conserving mutation R1073K abolished thermal activation (Supplementary Fig. S5*D*).

In light of these results, we also attempted to confer heat sensitivity to hTRPA1 by introducing the above point mutations and by exchanging the fifth and sixth transmembrane domains from dTRPA1. We were not able to record heat-activated currents from these channels (data not shown). This indicates that while replacement of the full transmembrane region of dTRPA1 into hTRPA1 (HDH) is sufficient for heat sensitivity, smaller substitutions require additional elements to maintain functionality.

## Residues in S4 set the temperature activation threshold of *Drosophila* transient receptor potential A1

Strikingly, all temperature insensitive mutants displayed normal voltage sensitivity implying that the thermal and voltage sensors are separate entities. To investigate this further, we sought to identify residues involved in voltage-dependent gating of dTRPA1. We neutralized all positively charged amino acids in the transmembrane region of dTRPA1 (Supplementary Fig. S6*A*) and determined the apparent gating charge ($Z_{app}$) and $V_{1/2}$ from the activation curve (Supplementary Fig. S6*B*). Surprisingly, none of the mutations altered $Z_{app}$; however, H990A-R1004N and H990Q-R1004A exhibited significantly higher $V_{1/2}$ values than dTRPA1 at 32°C (Fig. 6*A* and *B*) (dTRPA1: $63.5 \pm 3.4$ mV; H990A-R1004N: $80.3 \pm 12$ mV; H990Q-R1004A: $99.9 \pm 11.9$ mV). We examined thermal activation of these mutants by applying temperature ramps from 20°C to 46°C (Fig. 6*C* and *D*). H990A-R1004N and H990Q-R1004A were both responsive to heat, but thermal activation thresholds and half-maximal temperatures ($T_{1/2}$) were significantly increased compared to dTRPA1 ($T_{1/2}$ at 100 mV; dTRPA1: $25.2 \pm 0.2$°C; H990A-R1004N: $37.7 \pm 0.2$°C; H990Q-R1004A: $36.1 \pm 0.2$°C). Thus, selective perturbation of positively charged residues in S4 leads to an increase in the threshold for activation of the channel by voltage and temperature.

## Single channel analysis of *Drosophila* transient receptor potential A1 and mutant channels

To understand mechanistically how temperature gates TRP channels we undertook a single channel analysis of dTRPA1 and key mutants. We sought to develop a kinetic model of channel activation by temperature, reasoning that this would allow us to gain insight into gating mechanisms and potentially to correlate molecular perturbations arising from mutations with kinetic states. To this end we investigated single native dTRPA1 channels, the S4 mutant H990A-R1004N, and the temperature insensitive chimera dTRPA1–56H.

Consistent with whole cell recordings, single dTRPA1 channels activated more readily at higher temperatures (Fig. 7*A*) and assumed open and closed states with a peak current amplitude of 4.5 pA at 100 mV and 25°C (Supplementary Fig. S7*E*). Unitary current amplitude had a linear relationship with voltage (conductance of 41 ± 2 pS, Supplementary Fig. S7*F*) implying that the outward rectification seen in whole cell recordings can be ascribed to voltage sensitivity.

In cell-attached patches, dTRPA1 single channel traces were characterized by prolonged periods of inactivity punctuated by brief burst-like openings (Fig. 7*A*). We quantified activity by plotting dwell-time histograms for closed and open states at 24°C and 32°C. Histograms were well described by five closed and two open components (Fig. 7*B*–*E*), and the major effect of temperature was to shorten the duration of closed times (Fig. 7*F* and *G*). We further explored how these components were configured using a maximum likelihood approach to fit all possible non-cyclic models with five closed and two open states, and ranking each according to its log likelihood (LL) value. The higher ranking models all had uncoupled open states with at least two independent pathways between open and closed states (Supplementary

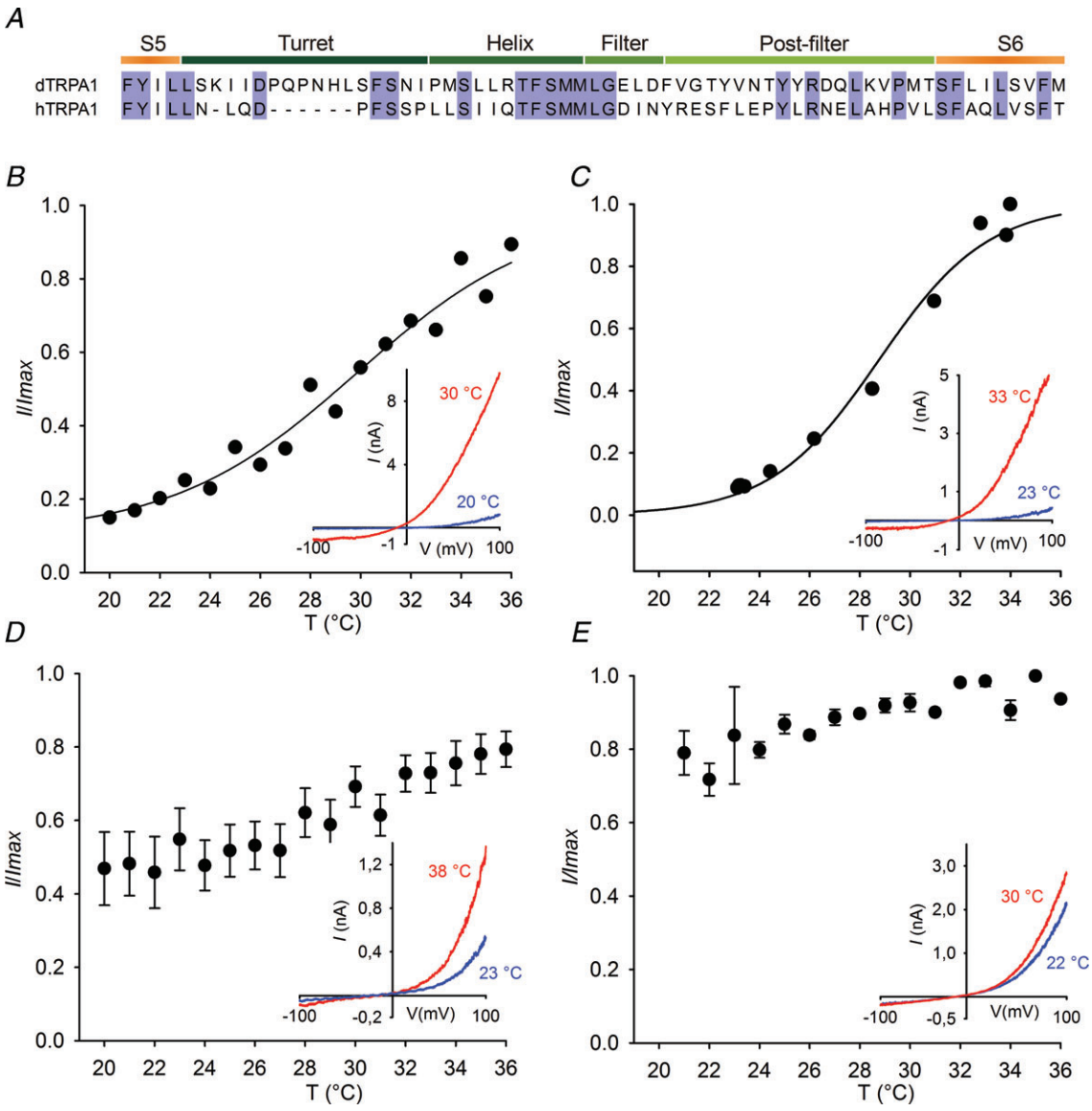


**Figure 4. Mapping the pore region of dTRPA1 for the thermoregulatory module**
*A*, sequence alignment of dTRPA1 and hTRPA1. Replacement of the putative pore turret (*B*) or sequence between the filter and S6 (*C*) in HDH does not reduce heat sensitivity. *D*, substitution of HDH S6 with human S6 or replacement of the pore helix (*E*) reduces heat sensitivity. Currents were normalized to peak current at +100 mV. Insets show representative *I–V* curves. dTRPA1, *Drosophila* transient receptor potential A1; hTRPA1, human TRPA1.

Table S1). Of these, Scheme 1 gave the best LL value and was characterized by an additional entry/exit state from one of the open states ($O_2 \rightarrow C_3$) (Fig. 7*H*). Interestingly, all of the higher ranking models shared several kinetic features. For example, one closed state ($C_5$) with low rate values ($<10\,s^{-1}$) was present in all models. In addition, the $C_1$ to $O_1$ equilibrium was shifted towards the open state and might account for the sporadic ongoing activity of dTRPA1 observed at 24°C.

We next investigated the effects of increasing temperature on model arrangement and kinetic behaviour. At 32°C, a similar model ranking was obtained as at 24°C and Scheme 1 reported the highest LL values. Estimated rate constants between states were however altered by heating (Fig. 7*I*). Transitions towards the pre-open state $C_2$ from $C_1$ and $C_4$, and to $O_2$ from $C_3$ were most sensitive to temperature, with the $C_3$ to $O_2$ transition undergoing a reversal in equilibrium towards the open state. These changes would serve to drive the gating towards the $O_2$ state upon heating suggesting that this is the major thermal activation pathway in dTRPA1.

To obtain further understanding of the molecular substrates associated with the dTRPA1 kinetic model, we applied a similar analysis to the S4 (H990A-R1004N) mutant channel. In whole cell recordings this mutant required higher temperature and voltage for activation (Fig. 6*A* and *C*). We therefore carried out single channel kinetic analysis at temperatures of 34°C and 40°C to parallel the levels of activity recorded with dTRPA1.

Single channel traces of H990A-R1004N were remarkably different to dTRPA1, and were characterized by the emergence of two clearly discernible open states at 2.1 pA and 4.5 pA, which we attributed to sub-conducting (S) and fully open channels (O) (Fig. 8*A* and Supplementary Fig. S7*G*). (In generating dwell-time histograms and kinetic models, we therefore undertook two parallel analyses where we first pooled the sub-conductance state with the open state, and secondly accounted for it as a separate state while idealizing data. In all cases, considering the subconductance as a discrete state produced better fits of the data and we thus focused on this approach.

Exponential fits of dwell-time histograms of H990A-R1004N indicated that it enters a minimum of four closed states, two subconductance states and two fully open states at 34°C and 40°C (Fig. 8*B*–*G*). Despite the emergence of the novel subconductance state, the principal effect of increased temperature on H990A-R1004N was to shorten the duration of closed times as observed

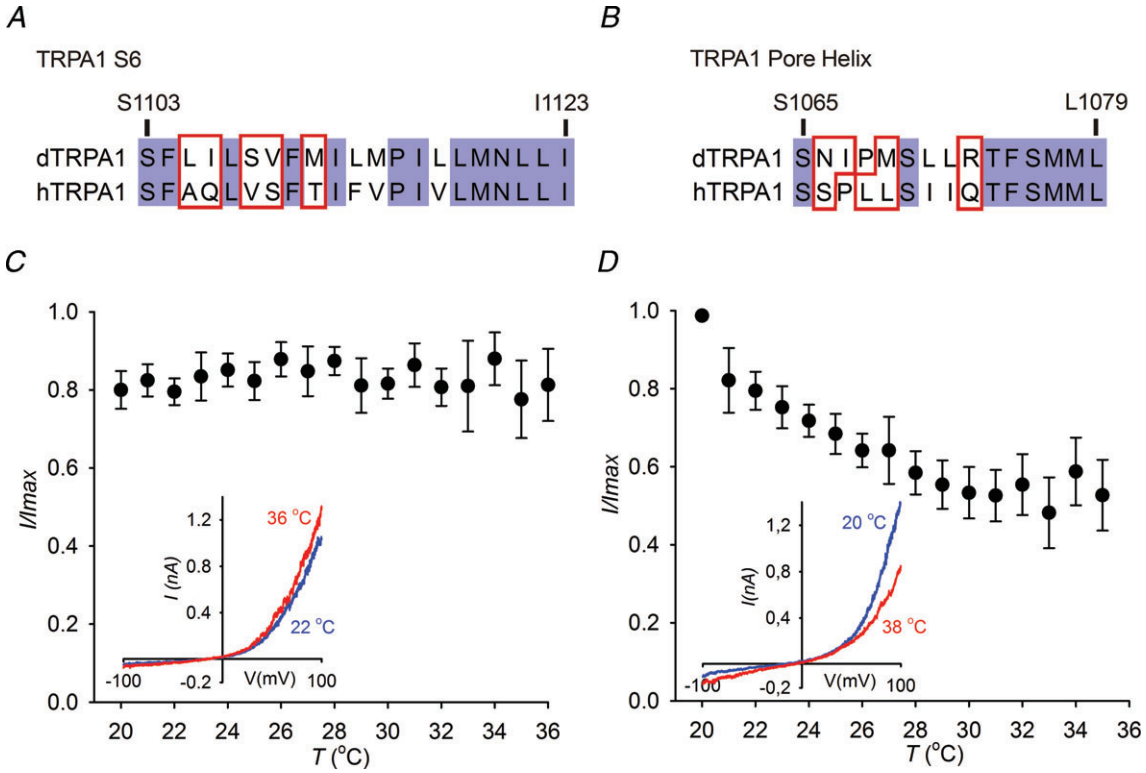


**Figure 5. Point mutations in S6 and the pore helix of *Drosophila* transient receptor potential A1 (dTRPA1) reverse heat sensitivity**
*A*, alignment of the S6 region (*A*) and pore helix (*B*) of dTRPA1 and hTRPA1. *C*, the mutation L1105A+I1106Q in S6 of HDH abolishes heat sensitivity. *D*, the HDH pore helix mutant, R1073Q is cold sensitive.

for wild-type dTRPA1 channels (Supplementary Fig. S7*I* and *J*). The configuration of the H990A-R1004N kinetic scheme was also analogous to dTRPA1 with the highest ranking models (Supplementary Table 1) having coupled closed states that transitioned through at least two gateway states to the open states. Similarly, increased temperature accelerated forward rates from all closed states towards $S_2$ and $O_2$ while simultaneously reducing the time spent in the $O_1$ state (Fig. 8*H* and Supplementary Table S1).

The kinetic scheme of H990A-R1004 also gives a number of valuable insights into the raised voltage and thermal thresholds of this mutant in whole cell recordings. For example, in all schemes, the subconductance states are positioned between closed and open states, indicating that they function as intermediate transitions required for entry to, or exit from, the open state. Potentially, these transitions could arise from instability of adjacent closed or open states, and serve to raise the energy barrier for full channel opening. It is also apparent that the $C_1$ to $O_1$ transition that is active in dTRPA1 at lower temperatures is not present in H990A-R1004N. Indeed, at 34°C the H990A-R1004N reaction scheme is dominated by backward transitions driving the gating towards the closed states $C_2$ and $C_3$.

From examining individual rate constants in the kinetic schemes of dTRPA1 and H990A-R1004N, it is not immediately apparent whether these models would fully account for the temperature dependency of the channels. To test this assumption we performed simultaneous fitting of data acquired at different temperatures, and estimated the temperature dependence of each rate constant (Supplementary Fig. S8*A*). These parameters were then used to simulate single channel currents arising from a slow temperature ramp from 15°C to

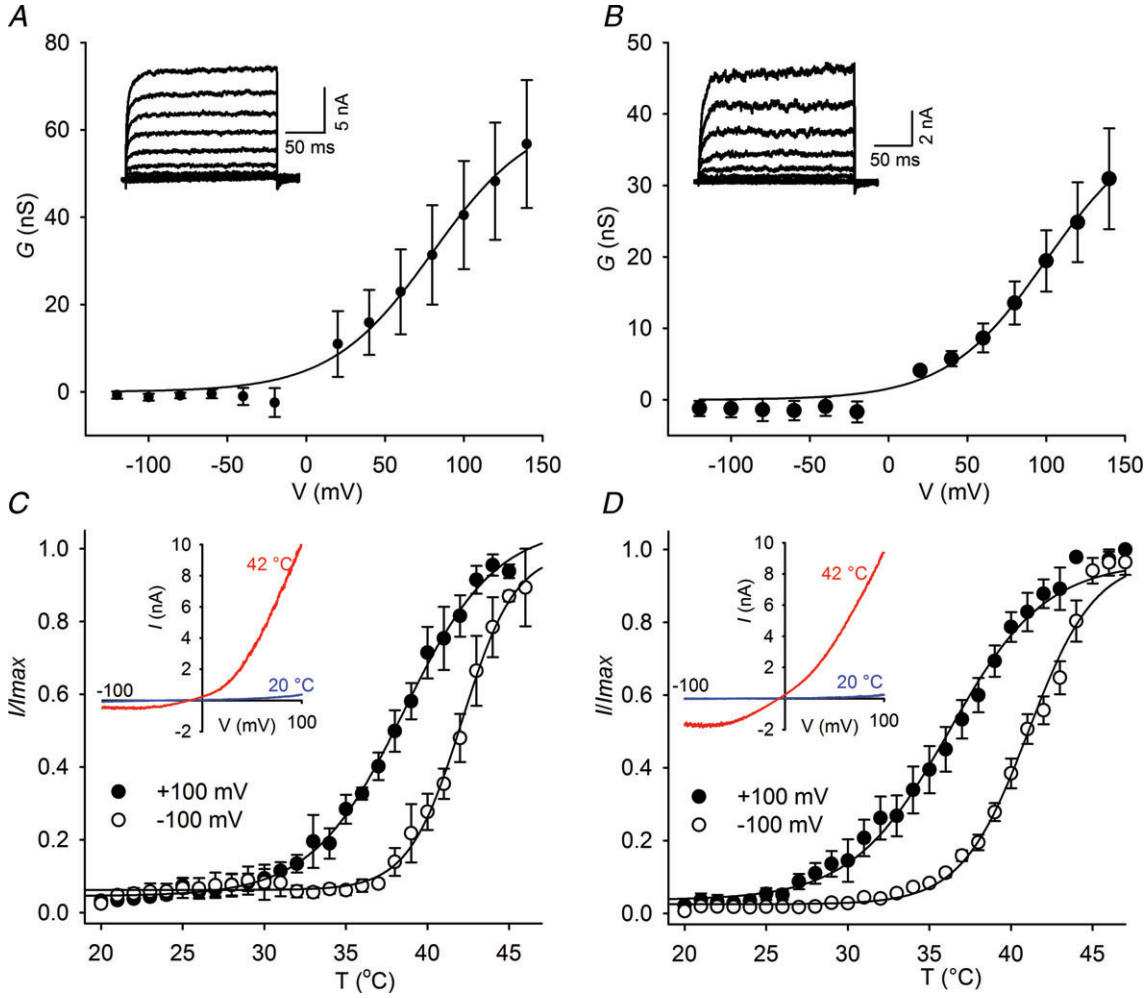


**Figure 6. Charge neutralizing mutations in S4 alter the temperature dependence of *Drosophila* transient receptor potential A1**
*A*, voltage-dependent activation of H990A-R1004N ($n = 5$) (*A*) and H990Q-R1004A ($n = 4$) (*B*) at 32°C. (Insets show representative whole cell current traces at 32°C in response to the voltage protocol indicated in Fig. 2*D*.) *C*, the H990A-R1004N ($n = 4$) and (*D*) H990Q-R1004A ($n = 6$) mutants have a higher temperature activation threshold.

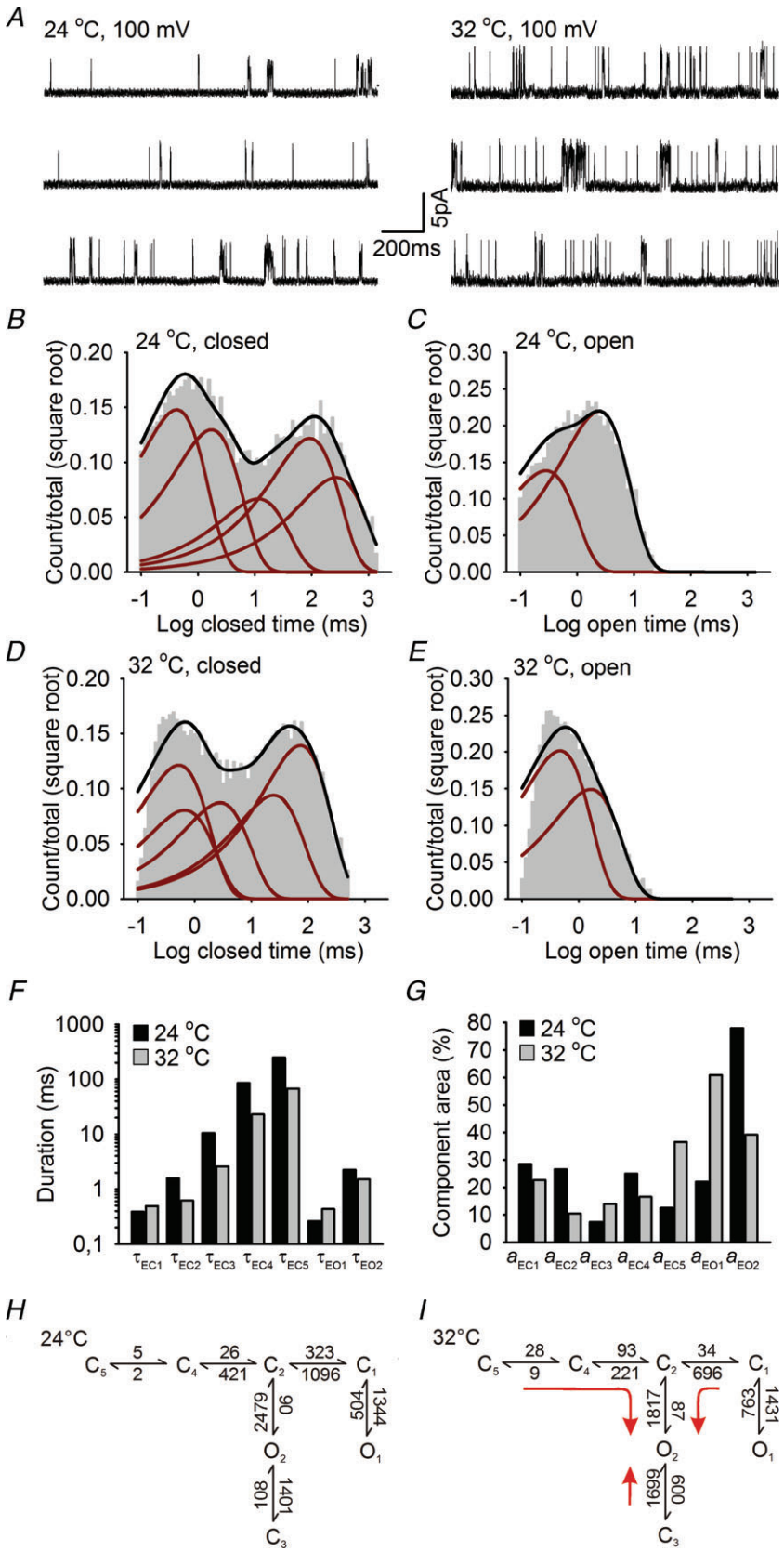


**Figure 7. Single channel analysis of *Drosophila* transient receptor potential A1 (dTRPA1)**
*A*, examples of dTRPA1 single channel currents recorded at +100 mV and 24°C and 32°C. *B–E*, histograms of dTRPA1 closed (*B*) and open distributions (*C*) at 24°C and 32°C (*D* and *E*). Histograms are superimposed with the probability density function (black line) and exponential components (red lines) estimated from fits of a five closed and two open state model. *F* and *G*, time constants (*F*) and areas (*G*) for the corresponding exponential components of closed (EC1–EC5) and open (EO1–EO2) distributions at 24°C and 32°C. *H* and *I*, highest ranking kinetic models of dTRPA1 single channel activity at 24°C and 32°C. Rates are in $s^{-1}$, red arrows indicate the principal transitions upon heating.

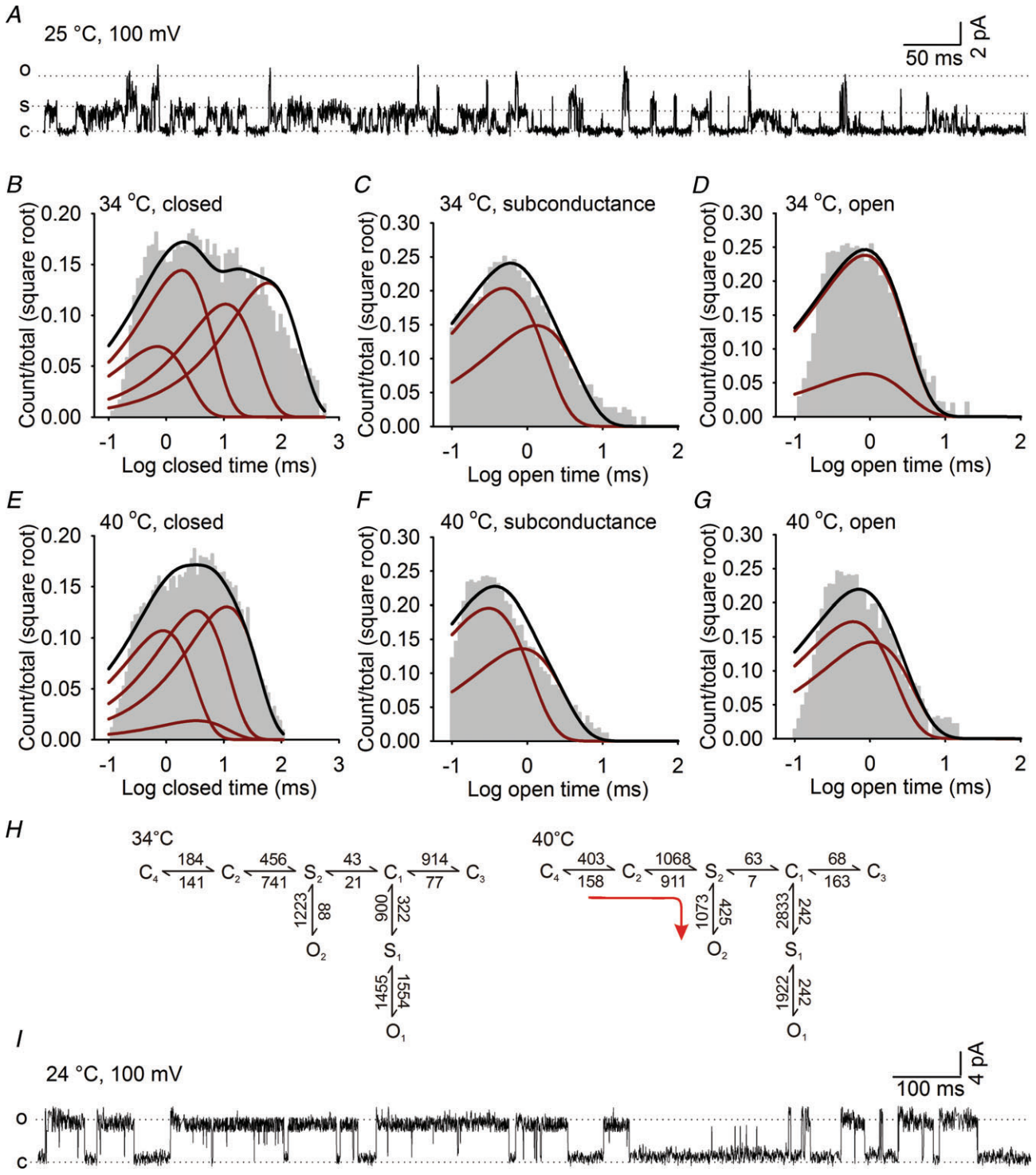


**Figure 8. Kinetic analysis of mutant *Drosophila* transient receptor potential A1 (dTRPA1) channels**
*A*, example of single channel currents of the S4 mutant (H990A-R1004N) recorded at +100 mV and 25°C. *B–G*, dwell-time histograms of closed (*B* and *E*), subconductance (*C* and *F*) and fully open states (*D* and *G*) for the H990A-R1004N mutant at 34°C and 40°C. The distributions are fitted with exponential components (red lines) derived from a five closed, two subconductance and two open state model and overlaid with the probability density function (black lines). *H*, highest ranking kinetic models of H990A-R1004N single channel activity at 34°C and 40°C. Rates are in $s^{-1}$, red arrows indicate the principal transitions upon heating. *I*, representative single channel trace of the dTRPA1–56H chimera at +100 mV and 25°C. *J* and *K*, histograms of dTRPA1–56H closed (*J*) and open distributions (*K*) fitted with exponential components (red lines) estimated from a four closed and four open state model (*I*).

45°C (0.2°C $s^{-1}$). As illustrated in Supplementary Fig. 8*B*, raising temperature increased channel activity for both dTRPA1 and H990A-R1004N. Moreover, the threshold for activation of H990A-R1004N was elevated with respect to dTRPA1 indicating that these models do indeed approximate the experimental data.

Finally, we wished to apply a kinetic analysis to a temperature-insensitive mutant channel. We initially recorded single channel traces from the R1073Q mutant; however, instability of the channel precluded a kinetic analysis (Supplementary Fig. S7*C*). We therefore focused on the dTRPA1–56H channel. This chimera had larger peak single channel current amplitude than dTRPA1 and H990A-R1004N (6.1 pA at 100 mV and 24°C, Supplementary Fig. S7*H*), and activity was characterized by bursts of long openings (Fig. 8*I*) with distributions dominated by brief closures and long openings (Fig. 8*J* and *K*). Histograms were fit by four closed and four open exponential components, and model fitting demonstrated that states preferentially arranged in a linear configuration (Figure 8*L* and Supplementary Table S1). Thus replacement of the pore region in dTRPA1 leads to a striking transformation of the gating scheme and single channel behaviour in dTRPA1–56H, which presumably underlies the temperature insensitivity and slow deactivation kinetics of this mutant in whole cell recordings.

## Discussion

The evolution of TRPA channels as cold or heat sensors across different species suggests they contain common elements in their structure and organization that allow them to be gated by temperature. Here, we have mapped heat-sensitive regions in *Drosophila* TRPA1 channels by analysing chimeric channels assembled from distinct functional units of human and *Drosophila* channels. We identified residues in the transmembrane region of *Drosophila* TRPA1 that are required for thermal activation of the channel, and from single channel recordings, we provide mechanistic insight into this process.

Previous studies have defined a number of different regions that govern thermosensitivity of TRP channels. Thermoregulatory elements have been described in the C-terminus (Brauchi *et al.* 2006), pore region (Grandl *et al.* 2008, 2010; Yang *et al.* 2010; Cui *et al.* 2012) and N-terminus (Yao *et al.* 2011) of mammalian TRP channels, implying that heat sensitivity may be a property that depends upon multiple structural units in different subtypes of TRP channels. Recently, TRPA1 has been the focus of several studies that have identified thermoregulatory modules in non-overlapping regions of the N-terminus of the channel. From analyses of alternatively spliced isoforms of dTRPA1, variations in the sequence of the distal N-terminus (Kang *et al.* 2012), and of the region flanking the ankyrin repeats (Zhong *et al.* 2012), have been demonstrated to modulate the thermosensitivity of isoforms. Similarly, heat-sensitive modules have been identified in rattlesnake TRPA that locate to the ankyrin-repeat domains and integrate diverse physiological signals (Cordero-Morales *et al.* 2011). While we found that the N-terminus of dTRPA1 does not influence heat sensitivity of chimeric channels, it is possible that chimeras comprising the full *Drosophila* N-terminus might not recapitulate the phenotype of smaller insertions within this region. Moreover, an inherent limitation of the approach used in these and our study is that it is not possible to determine whether mutations affect temperature sensing or temperature gating. It is likely that thermal activation of TRP channels will not rely upon a single domain, but instead involves the concerted action of multiple units that detect, integrate and transduce thermal stimuli to ultimately gate the channel. This interpretation would explain the apparent discrepancy in results from several different studies.

Our data points towards a role for the pore region of dTRPA1 in setting thermosensitivity. This region has been implicated as a key integrator for multiple stimuli in TRPV channels (Kuzhikandathil *et al.* 2001; Susankova

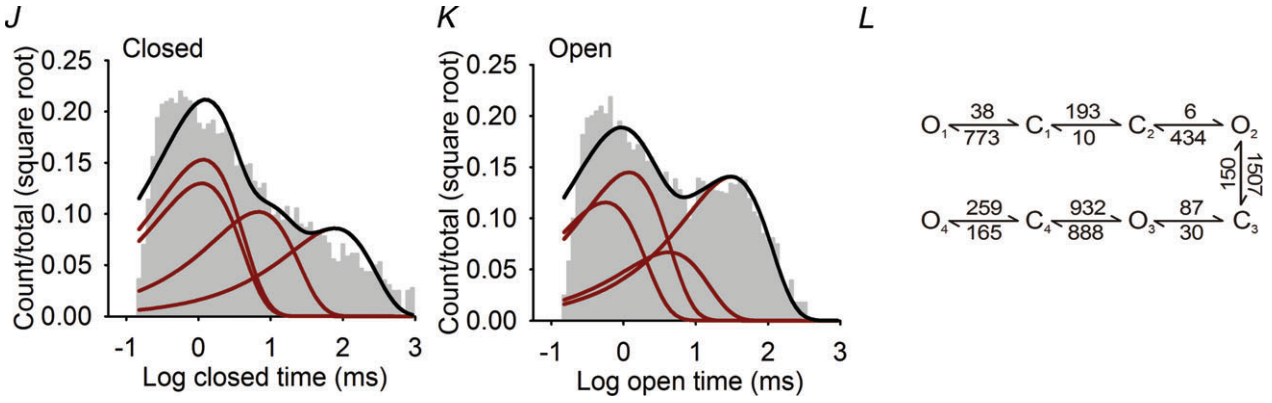


**Figure 8.** Continued.

*et al.* 2007; Grandl *et al.* 2008, 2010; Myers *et al.* 2008; Yang *et al.* 2010; Aneiros *et al.* 2011; Cui *et al.* 2012), and the location of all heat-insensitive substitutions to S6 and the pore helix in dTRPA1, suggests that mutations here affect the final steps of the thermal activation pathway. In TRPV1, the S6 segment forms the activation gate of the channel allowing access to the pore (Salazar *et al.* 2009). This region in TRPA1 channels is particularly well conserved and significant divergence between human and *Drosophila* sequence occurs only before a proline residue at position 1115 (Fig. 5*A*). Proline is also present at the same position in voltage-gated potassium channels and functions as a 'hinge' allowing flexibility of S6 and opening of the channel (Catterall, 2010). An intriguing possibility is that S6 has a similar function in dTRPA1 and couples the heat sensing apparatus to channel opening.

Several lines of evidence support a role for the pore loop in thermal activation of TRP channels. In TRPV channels, mutations in the pore turret and extracellular loop that follows the selectivity filter reduce heat sensitivity (Grandl *et al.* 2008, 2010; Yang *et al.* 2010; Cui *et al.* 2012). We observed that exchange of these regions in dTRPA1 with human sequence did not alter thermal activation. Thus, TRPA channels may either use a different mechanism for temperature sensing, or point mutagenesis here exerts secondary effects on channel structure that were not evident in chimeric channels. In contrast, we found that the putative pore helix is required for temperature sensitivity. Replacement of *Drosophila* sequence with its human counterpart abolished heat activation, implying that the structure of the dTRPA1 pore permits gating by temperature and is a critical part of the thermal activation pathway.

Notably, none of the temperature-insensitive mutants in the pore helix or S6 displayed a temperature-dependent shift in voltage activation, although basal voltage dependence was retained. This argues against a single sensor for voltage and temperature and instead suggests that coupling between voltage and temperature sensors is disrupted in these mutants. Intriguingly, we did identify two residues in the S4 domain of dTRPA1 that elevated both voltage and temperature thresholds. This region functions as a core voltage sensing module in voltage-gated potassium channels (Catterall, 2010), and has been implicated in voltage sensing in TRPM8 (Voets *et al.* 2007), suggesting that S4 could have a similar function in dTRPA1. However, the observation that charge neutralizing mutations in this region did not alter $Z_{app}$ implies that these residues do not regulate voltage sensitivity directly but instead may exert allosteric effects on the stability of open or closed states.

Single channel analysis allowed us to explore these assumptions in more detail and to define the gating reaction of dTRPA1 and key mutants. In broad agreement with a recent study on single TRPM8 channels (Fernandez *et al.* 2011), we found that dTRPA1 single channel activity was well described by a five closed and two open state kinetic model and that the predominant effect of heating was to shorten closed distribution times. Of note, it has been proposed that thermal activation of TRPV1 is dependent upon long duration openings, which are absent in temperature-insensitive mutants (Grandl *et al.* 2010). We did not observe long open dwell-times in dTRPA1, suggesting that this mechanism may not be a general requirement for temperature sensitivity of TRP channels.

Our analysis of single mutant dTRPA1 channels enabled us to ascribe kinetic events with molecular perturbations that alter channel thermosensitivity. We initially examined the S4 mutant, H990A-R1004N, which displayed elevated voltage and temperature activation thresholds in whole cell recordings. Single channel analysis revealed that this channel had dramatically different properties to wild-type dTRPA1. From the H990A-R1004N kinetic scheme, two features are immediately apparent; first the emergence of a subconductance that precedes transition into open states, and secondly the dominance of backward transitions driving the gating toward closed states. We propose that the subconductance reflects a transition in channel gating that is not detectable in wild-type dTRPA1, and arises from instability of the open states. Together with backward transitions this would raise the energy barrier for full channel opening and thus account for the reduced voltage and temperature sensitivity observed in whole cell recordings.

Analysis of the temperature-insensitive chimera dTRPA1–56H also gave valuable insights into thermal activation of dTRPA1. At the single channel level, this chimera displayed a striking alteration in behaviour compared to wild-type channel such that recordings were dominated by long openings and kinetic schemes favoured a linear configuration. These data indicate that the pore of TRPA1 incorporates the functional units that define the gating scheme, and that the evolution of this region in human and *Drosophila* TRPA1 has produced channels with entirely different gating mechanisms. Based upon these observations, we speculate that the configuration of the gating reaction, and the temperature dependence of individual transitions within each scheme, underlie the differential thermosensitivity of human and *Drosophila* TRPA1 and dictate whether the channel will respond to cooling or heating. Further analysis of more subtle mutations in dTRPA1 and other TRP channels will allow for the testing of this hypothesis and a better understanding of how temperature is detected and promotes channel opening.

We have mapped thermo-responsive domains in dTRPA1 using a strategy based upon the analysis of chimeric *Drosophila* and human TRPA1 channels. Our approach raises a fundamental question as to how human and fly channels acquired opposite temperature sensitivity

from an evolutionary perspective. Did mammalian TRPA1 channels convert an ancestral warm activated channel into a cold sensor, or did insect, snake and mammalian channels acquire thermal sensitivity independently? We show that very few amino acids must be mutated to render a hot channel cold sensitive, supporting the idea that a small change in sequence could permit the evolution of cold sensing mammalian channels from a heat responsive ancestor. Further investigation into the functional properties of TRPA1 orthologues in other species and ultimately a structural description of TRP channels will provide an evolutionary basis for temperature sensitivity of these channels.

## References


Aneiros E, Cao L, Papakosta M, Stevens EB, Phillips S & Grimm C (2011). The biophysical and molecular basis of TRPV1 proton gating. *EMBO J* **30**, 994–1002.

Bandell M, Story GM, Hwang SW, Viswanath V, Eid SR, Petrus MJ, Earley TJ & Patapoutian A (2004). Noxious cold ion channel TRPA1 is activated by pungent compounds and bradykinin. *Neuron* **41**, 849–857.

Barry PH & Diamond JM (1970). Junction potentials, electrode standard potentials, and other problems in interpreting electrical properties of membranes. *J Membr Biol* **3**, 93–122.

Bautista DM, Jordt SE, Nikai T, Tsuruda PR, Read AJ, Poblete J, Yamoah EN, Basbaum AI & Julius D (2006). TRPA1 mediates the inflammatory actions of environmental irritants and proalgesic agents. *Cell* **124**, 1269–1282.

Brauchi S, Orio P & Latorre R (2004). Clues to understanding cold sensation: thermodynamics and electrophysiological analysis of the cold receptor TRPM8. *Proc Natl Acad Sci U S A* **101**, 15494–15499.

Brauchi S, Orta G, Salazar M, Rosenmann E & Latorre R (2006). A hot-sensing cold receptor: C-terminal domain determines thermosensation in transient receptor potential channels. *J Neurosci* **26**, 4835–4840.

Catterall WA (2010). Ion channel voltage sensors: structure, function, and pathophysiology. *Neuron* **67**, 915–928.

Cordero-Morales JF, Gracheva EO & Julius D (2011). Cytoplasmic ankyrin repeats of transient receptor potential A1 (TRPA1) dictate sensitivity to thermal and chemical stimuli. *Proc Natl Acad Sci U S A* **108**, E1184–1191.

Cui Y, Yang F, Cao X, Yarov-Yarovoy V, Wang K & Zheng J (2012). Selective disruption of high sensitivity heat activation but not capsaicin activation of TRPV1 channels by pore turret mutations. *J Gen Physiol* **139**, 273–283.

Fernandez JA, Skryma R, Bidaux G, Magleby KL, Scholfield CN, McGeown JG, Prevarskaya N & Zholos AV (2011). Voltage- and cold-dependent gating of single TRPM8 ion channels. *J Gen Physiol* **137**, 173–195.

Gracheva EO, Ingolia NT, Kelly YM, Cordero-Morales JF, Hollopeter G, Chesler AT, Sanchez EE, Perez JC, Weissman JS & Julius D (2010). Molecular basis of infrared detection by snakes. *Nature* **464**, 1006–1011.

Grandl J, Hu H, Bandell M, Bursulaya B, Schmidt M, Petrus M & Patapoutian A (2008). Pore region of TRPV3 ion channel is specifically required for heat activation. *Nat Neurosci* **11**, 1007–1013.

Grandl J, Kim SE, Uzzell V, Bursulaya B, Petrus M, Bandell M & Patapoutian A (2010). Temperature-induced opening of TRPV1 ion channel is stabilized by the pore domain. *Nat Neurosci* **13**, 708–714.

Hamada FN, Rosenzweig M, Kang K, Pulver SR, Ghezzi A, Jegla TJ & Garrity PA (2008). An internal thermal sensor controlling temperature preference in Drosophila. *Nature* **454**, 217–220.

Jordt SE, Bautista DM, Chuang HH, McKemy DD, Zygmunt PM, Hogestatt ED, Meng ID & Julius D (2004). Mustard oils and cannabinoids excite sensory nerve fibres through the TRP channel ANKTM1. *Nature* **427**, 260–265.

Jordt SE, McKemy DD & Julius D (2003). Lessons from peppers and peppermint: the molecular logic of thermosensation. *Curr Opin Neurobiol* **13**, 487–492.

Kang K, Panzano VC, Chang EC, Ni L, Dainis AM, Jenkins AM, Regna K, Muskavitch MA & Garrity PA (2012). Modulation of TRPA1 thermal sensitivity enables sensory discrimination in Drosophila. *Nature* **481**, 76–80.

Kang K, Pulver SR, Panzano VC, Chang EC, Griffith LC, Theobald DL & Garrity PA (2010). Analysis of Drosophila TRPA1 reveals an ancient origin for human chemical nociception. *Nature* **464**, 597–600.

Karashima Y, Talavera K, Everaerts W, Janssens A, Kwan KY, Vennekens R, Nilius B & Voets T (2009). TRPA1 acts as a cold sensor in vitro and in vivo. *Proc Natl Acad Sci USA* **106**, 1273–1278.

Kuzhikandathil EV, Wang H, Szabo T, Morozova N, Blumberg PM & Oxford GS (2001). Functional analysis of capsaicin receptor (vanilloid receptor subtype 1) multimerization and agonist responsiveness using a dominant negative mutation. *J Neurosci* **21**, 8697–8706.

Lee Y, Lee J, Bang S, Hyun S, Kang J, Hong ST, Bae E, Kaang BK & Kim J (2005). Pyrexia is a new thermal transient receptor potential channel endowing tolerance to high temperatures in Drosophila melanogaster. *Nat Genet* **37**, 305–310.

McKemy DD (2007). Temperature sensing across species. *Pflugers Arch* **454**, 777–791.

Myers BR, Bohlen CJ & Julius D (2008). A yeast genetic screen reveals a critical role for the pore helix domain in TRP channel gating. *Neuron* **58**, 362–373.

Nilius B, Talavera K, Owsianik G, Prenen J, Droogmans G & Voets T (2005). Gating of TRP channels: a voltage connection? *J Physiol* **567**, 35–44.

Patapoutian A, Peier AM, Story GM & Viswanath V (2003). ThermoTRP channels and beyond: mechanisms of temperature sensation. *Nat Rev Neurosci* **4**, 529–539.

Qin F (2004). Restoration of single-channel currents using the segmental k-means method based on hidden Markov modelling. *Biophys J* **86**, 1488–1501.

Qin F, Auerbach A & Sachs F (1997). Maximum likelihood estimation of aggregated Markov processes. *Proc Biol Sci* **264**, 375–383.

Salazar H, Jara-Oseguera A, Hernandez-Garcia E, Llorente I, Arias O, II, Soriano-Garcia M, Islas LD & Rosenbaum T (2009). Structural determinants of gating in the TRPV1 channel. *Nat Struct Mol Biol* **16**, 704–710.

Story GM, Peier AM, Reeve AJ, Eid SR, Mosbacher J, Hricik TR, Earley TJ, Hergarden AC, Andersson DA, Hwang SW, McIntyre P, Jegla T, Bevan S & Patapoutian A (2003). ANKTM1, a TRP-like channel expressed in nociceptive neurons, is activated by cold temperatures. *Cell* **112**, 819–829.

Susankova K, Ettrich R, Vyklicky L, Teisinger J & Vlachova V (2007). Contribution of the putative inner-pore region to the gating of the transient receptor potential vanilloid subtype 1 channel (TRPV1). *J Neurosci* **27**, 7578–7585.

Talavera K, Yasumatsu K, Voets T, Droogmans G, Shigemura N, Ninomiya Y, Margolskee RF & Nilius B (2005). Heat activation of TRPM5 underlies thermal sensitivity of sweet taste. *Nature* **438**, 1022–1025.

Tracey WD, Jr., Wilson RI, Laurent G & Benzer S (2003). painless, a Drosophila gene essential for nociception. *Cell* **113**, 261–273.

Viswanath V, Story GM, Peier AM, Petrus MJ, Lee VM, Hwang SW, Patapoutian A & Jegla T (2003). Opposite thermosensor in fruitfly and mouse. *Nature* **423**, 822–823.

Voets T, Droogmans G, Wissenbach U, Janssens A, Flockerzi V & Nilius B (2004). The principle of temperature-dependent gating in cold- and heat-sensitive TRP channels. *Nature* **430**, 748–754.

Voets T, Owsianik G, Janssens A, Talavera K & Nilius B (2007). TRPM8 voltage sensor mutants reveal a mechanism for integrating thermal and chemical stimuli. *Nat Chem Biol* **3**, 174–182.

Yang F, Cui Y, Wang K & Zheng J (2010). Thermosensitive TRP channel pore turret is part of the temperature activation pathway. *Proc Natl Acad Sci U S A* **107**, 7083–7088.

Yao J, Liu B & Qin F (2011). Modular thermal sensors in temperature-gated transient receptor potential (TRP) channels. *Proc Natl Acad Sci U S A* **108**, 11109–11114.

Zhong L, Bellemer A, Yan H, Honjo K, Robertson J, Hwang RY, Pitt GS & Tracey WD (2012). Thermosensory and non-thermosensory isoforms of Drosophila melanogaster TRPA1 reveal heat sensor domains of a thermoTRP channel. *Cell Rep* **1**, 43–55.

Zurborg S, Yurgionas B, Jira JA, Caspani O & Heppenstall PA (2007). Direct activation of the ion channel TRPA1 by $Ca^{2+}$. *Nat Neurosci* **10**, 277–279.

## Author contributions

H.W. designed and performed experiments. M.S. and S.Z. assisted with experiments. P.H. initiated and supervised the project and wrote the manuscript with discussion from all authors. Experiments were performed at EMBL Monterotondo. All authors approved the final version of the manuscript.

## Acknowledgements

We thank C. Martinez and G. Onjaro for technical assistance, B. Yurgionas for assistance with calcium imaging, and A. Patapoutian for providing the dTRPA1 cDNA. This work was supported by EMBL, the Deutsche Forschungsgemeinschaft (S.Z.) and the Ernst Schering Foundation (H.W.).